Liquid–Vapor Equilibria of Ionic Liquids from a SAFT Equation of State with Explicit Electrostatic Free Energy Contributions

ARTICLE *in* THE JOURNAL OF PHYSICAL CHEMISTRY B · APRIL 2015

Impact Factor: 3.3 · DOI: 10.1021/jp511571h · Source: PubMed

3 AUTHORS:

Orlando Guzmán

Metropolitan Autonomous University

40 PUBLICATIONS **413** CITATIONS

SEE PROFILE

Jesús Eloy Ramos Lara

1 PUBLICATION **0** CITATIONS

SEE PROFILE

Fernando Del Río

Universidad Autónoma Metropolitana, Mexico…

91 PUBLICATIONS **913** CITATIONS

SEE PROFILE

THE JOURNAL OF PHYSICAL CHEMISTRY B

Article

pubs.acs.org/JPCB

Liquid–Vapor Equilibria of Ionic Liquids from a SAFT Equation of State with Explicit Electrostatic Free Energy Contributions

Orlando Guzmán,*[,†] J. Eloy Ramos Lara,*[,†,‡] and Fernando del Río*[,†]

[†]Departamento de Física, Universidad Autónoma Metropolitana, Iztapalapa, Apdo 55 534, México DF 09340, México

[‡]Colegio de Ciencia y Tecnología, Universidad Autónoma de la Ciudad de México, México DF 09790, México

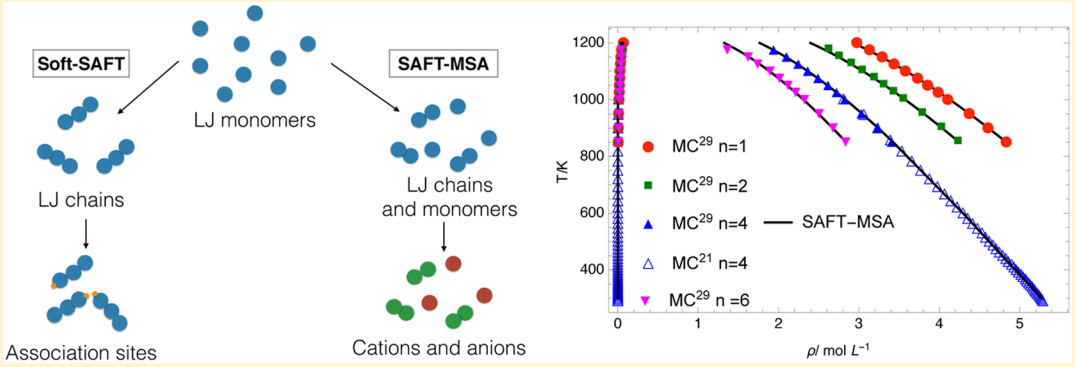

ABSTRACT: Statistically associating fluid theory (SAFT) provides closed-form free energies by perturbation methods. We propose here a SAFT equation of state for ionic liquids that models the contribution from Coulomb forces after that of the Restricted Primitive Model (RPM) in the Mean Spherical Approximation (MSA). The resulting SAFT-MSA equation, fitted to simulated orthobaric curves of imidazolium based ionic liquids, predicts experimental density data with errors ≈1% and the characteristic decrease of all critical coordinates with increasing cation size. The SAFT-MSA equation can be applied to calculate thermodynamic coefficients, the speed of sound and surface tension (among other properties) of pure ionic liquids and can be generalized straightforwardly to mixtures.

INTRODUCTION

Room temperature ionic liquids (RTILs) are salts that are liquid at standard pressure and temperatures below 100 °C. Since many RTILs are formed by organic constituents, it is possible to choose among a large variety of chemical structures for cations and anions, in order to fine-tune properties (such as thermal expansivity, viscosity, conductivity, or solubility of a given species) for a particular application. For instance, several RTILs have an extremely low vapor pressure,[1] which renders them nonvolatile, nonflammable, and nonexplosive; therefore, they are good candidates to replace organic volatile compounds as industrial solvents.[2,3] Room temperature ionic liquids have been called "designer solvents" and considered important substances for developing new separation processes.[2,4,5]

RTILs are typically stable at temperatures that are high compared with room temperature, but decompose at several hundreds of degrees Celsius.[6] Chemical decomposition prevents experimental access to their critical and supercritical states.[7] There are many published experimental determinations of RTIL properties, such as density and viscosity,[8,9] refractive index,[10] surface tension,[11] vapor pressure,[1] thermodynamic coefficients,[12] and speed of sound,[13] among others. A database of ionic liquid experimental publications, including numerical data, is available from NIST;[14] the update released on December 2013 included data for over a thousand ionic liquids (in pure, binary and ternary mixture systems). In spite of this, the sheer variety of cations and anions in ionic liquids makes it very important to develop theoretical avenues to predict their properties.

Among the theoretical approaches for the prediction of RTIL properties, we find molecular simulations,[15−21] group-contribution procedures (e.g., Joback's method[22] or newer approaches[23,24]), and equations of state (EOS) obtained by statistical-mechanics methods[25−28]

While EOS for thermodynamic potentials can be used to derive all thermodynamic properties, many widely used EOS for the pressure (like the Peng–Robinson or Redlich–Kwong equations) rely on prior knowledge of critical constants. Since RTIL critical coordinates are not directly measurable, this limits application of such equations to cases where the critical point can be determined reliably by molecular simulation,[19−21,29] or extrapolated from experimental data (for instance, from the temperature behavior of surface tension).[11]

Successful theories for the equation of state use molecular-based insights to build up closed-form expressions for thermodynamic potentials; they result in transferable models

Received: November 19, 2014
Revised: April 19, 2015
Published: April 20, 2015

DOI: 10.1021/jp511571h
J. Phys. Chem. B 2015, 119, 5864−5872

with regular behavior of their parameters, which have a clear molecular interpretation. Statistical associating fluid theory (SAFT) equations for the Helmholtz's free energy are of this kind: they are based on a perturbation-theory treatment of molecular association. In the limit of very strong association between monomers, one can represent in an unified way the formation of permanently bonded chain molecules and the transient, or statistical, association of already formed chains.

While the SAFT perturbation methodology is the same in all its variants, they differ in the precise system chosen as reference (e.g., Lennard−Jones, LJ, or hard sphere systems), as well as in the model and approximations used to represent dispersive interactions, chain-formation and association contributions. There is a review by Tan et al. of SAFT models applied to RTIL.[30] In general, the models can be classified in two large groups: (1) Those that assume a complete pairing of one cation with one ion, to form a neutral ionic-liquid molecule, and (2) those that consider the cation and anion to be not necessarily associated. Nevertheless, whereas the former assume full pairing, the latter do not really assume full dissociation because the Coulomb forces that they introduce can produce partial ion pairing.

One of the earliest works to apply the SAFT approach to RTIL was that of Kroon and co-workers, who used the truncated-perturbed-chain polar statistical associating fluid theory (tPC−PSAFT) EOS. In this EOS, the ions form cation−anion pairs, considered then as ionic-liquid molecules, and the model considers explicitly the dipolar interactions between distinct ionic liquid molecules.[31,32] In another approach that also considers ionic liquid molecules, Andreu and Vega introduced the soft-SAFT EOS for systems containing RTIL; they have used it to investigate the solubility of gases in RTIL,[33,34] and to predict the behavior of mixtures containing ionic liquids.[35] We discuss this work with more detail below. More recently, Paduszynski and co-workers have used perturbed-chain, PC-SAFT, to model the liquid−liquid phase equilibrium of ionic liquids plus organic molecules. They also assume full pairing between cation and anion.[36−39]

Lastly, we may mention the SAFT models with cations and ions not fully associated. In the work of Ji and Adidharma,[26] the heterosegmented statistical associating fluid theory, he-SAFT is used to calculate the density of several ionic liquids. Nevertheless, the cation and anion are not subjected to a Coulombic interaction but to cross association in localized sites. More recent articles by Ji and co-workers[40,41] introduced a model called ePC-SAFT in which the cation and anion are assumed to be separate charged entities, and their interaction therefore includes an electrostatic Debye−Hückel term in the Helmholtz free energy. This characteristic has a direct bearing on the model here proposed and thus will be commented further below.

The soft-SAFT model uses a Lennard−Jones fluid as its reference (a soft potential, in contrast to the hard core systems used in other SAFT variants) and parametrize it with a diameter σ and a dispersive energy ε. The RTIL is modeled as chains of m segments identified as the reference Lennard-Jones particles; each of the chains contains (at least) one association site characterized by an association energy ε_{assoc} and an association volume K_{assoc}. By fitting their model to experimental data for the standard-pressure density in a given range of temperature, Andreu and Vega obtained correlations for the soft-SAFT parameters as functions of the molecular weight of three families of RTIL (formed by imidazolium-based cations in combination with $[BF_4]$, $[PF_6]$, and $[Tf_2N]$ anions).

Using the soft-SAFT equation of state as presented and parametrized by Andreu and Vega,[33] we calculated the orthobaric curves for the RTIL family of 1-alkyl-3-methyl-imidazolium tetrafluoroborates, $[C_nmim][BF_4]$, see Figure 1.

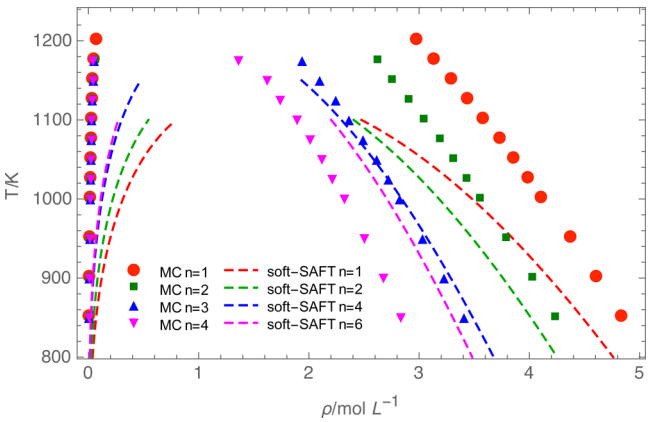

Figure 1. Orthobarics for the RTIL family $[C_nmim][BF_4]$ predicted by the soft-SAFT equation of Andreu and Vega[33] do not follow the regular behavior of the Monte Carlo simulation results of Rai and Maginn[29] (the error bars are smaller than the corresponding symbols). In the simulations (for n = 1, 2, 4, and 6), the saturated-liquid density decreases systematically as the cation's alkyl-chain size increases.

We found that the soft-SAFT EOS overestimates the vapor density and predicts an increase of the critical temperature with the size of the cation alkyl-chain size, which is contrary to what is observed in simulations.[21,29] Rai and Maginn found that the critical temperature, density and pressure decrease with C_n for the $[C_nmim][BF_4]$family. They also identified the decrease of the critical temperature as characteristic of ionic liquids, since nonionic fluids like alkanes and alcohols behave in the opposite way. A very low density of the saturated vapor is characteristic of ionic fluids (e.g., the Restricted Primitive Model or inorganic fused salts like sodium chloride) and an increase in the critical temperature for larger chains is common for nonionic fluids, even if they present association. In view of this situation, we developed a new SAFT model that includes an explicit contribution from electrostatic forces. With this new model we obtained better agreement with orthobaric curves and vaporization properties from simulation, while keeping excellent agreement with experimental data for standard-pressure densities.

Electrostatic interactions in electrolytes have been captured successfully within SAFT formalisms, such as the SAFT-VRE of Gil-Villegas and co-workers.[42] They analyzed the thermodynamics and phase equilibria of inorganic-salt aqueous solutions by building a SAFT equation of state from perturbation theory with a square-well reference. The usual SAFT-VR perturbation terms (corresponding to overlap and dispersion forces, chain formation, and intermolecular association) were included and the electrostatic interactions were then modeled by the Mean Spherical Approximation (MSA) results corresponding to the Restricted Primitive Model (RPM). A similar approach was followed by Tan et al.;[43] they coupled the SAFT1 equation of state with the restricted primitive model free-energy contribution from MSA. They considered that the RPM and the Primitive Model with different-sized ions give similar results,

DOI: 10.1021/jp511571h
J. Phys. Chem. B 2015, 119, 5864−5872

and modeled the electrolytes with a single, but state-dependent, diameter.

In work that was already mentioned, Ji and co-workers have modeled carbon dioxide and methane solubility in imidazolium-based RTIL, using several SAFT modeling strategies.[40,41] Some of these strategies are based on treating ion pairs effectively as molecules and including into the SAFT equation of state different combinations of dispersion, association and polar terms. The other strategies assume electrostatic interactions between ions and describe them through a Debye−Hückel term. Ji et al. report that they obtained best results with the second type of strategy.

In the new equation of state of this work, we do not include association terms in the free energy. Instead, we model the effect of Coulomb forces through the results of the mean spherical approximation for the Restricted Primitive Model; we refer to this new model as SAFT-MSA. Further, in order to assess the effect of corrections to the MSA approach, we added the so-called "truncated Γ2 approximation" correction proposed by Larsen et al.[44] We shall call this the SAFT-TΓ2A model. Contrary to the case of Debye−Hückel theory for dilute electrolytes, in using either SAFT-MSA or SAFT-TΓ2A we do not have to assume low charge carrier densities and, therefore, are able to describe simultaneously the gas and liquid phases.

We found that, without any association term, using the electrostatic MSA term improves the representation of simulated orthobaric curves for RTIL, while preserving the good agreement with experimental density data. Moreover, using this approach we reproduced the lowering of simulated critical temperatures of RTIL with increasing alkyl-chain size. We also obtained improvements over the soft-SAFT EOS results for the (simulation-derived) critical density and pressure, as well as the normal boiling-point temperature, entropy and latent heat of vaporization. Contrary to our expectations, the correction in the SAFT-TΓ2A equation did not improve significantly the results from the simpler SAFT-MSA model. For future work, we discuss the possibility of parametrizing the SAFT-MSA equation directly to experimental data on thermodynamic coefficients and different ways to generalize it to mixtures and accounting for different-sized ions.

In order to test further the SAFT-MSA model, we also treated two other RTIL imidiazolium-based families: One member of the series with the hexafluorophosphate anion, $[PF_6]$, and three members of the series with the bis-(trifluoromethylsulfonyl)amide anion, $[NTf_2]$. For these cases we obtained the orthobarics and the liquid densities at normal pressure, to be compared respectively with simulation results and experiments, as explained below.

METHODS

The SAFT-MSA model has three nonelectrostatic contributions: the ideal, reference, and chain terms, plus one electrostatic contribution given by the MSA treatment of the interactions in the Restricted Primitive Model:[43]

$$\beta a = \beta a_{\mathrm{Id}} + \beta a_{\mathrm{ref}} + \beta a_{\mathrm{chain}} + \beta a_{\mathrm{MSA}} \tag{1}$$

where $\beta = 1/k_B T$ and $a = A/N$ is the Helmholtz free energy per particle. For the sake of a simpler notation, we use molecular units by taking the parameters σ and ε as our length and energy units. This amounts to the use of reduced variables and dropping the customary asterisk that denotes them. In order to convert property values from molecular units to SI units, we denote values in the latter with a hat $\hat{()}$ and exhibit the molecular units as combinations of $\hat{\varepsilon}$, $\hat{\sigma}$, and the Boltzmann constant, namely, $\hat{T} = T\,\hat{\varepsilon}/k_B$, $\hat{\rho} = \rho/\hat{\sigma}^3$, $\hat{p} = p\hat{\varepsilon}/\hat{\sigma}^3$, $\hat{s} = k_B s$, $\hat{\varepsilon}_{\mathrm{ion}} = \varepsilon_{\mathrm{ion}}\,\hat{\varepsilon}$, $\hat{\kappa} = \kappa/\,\hat{\sigma}$, and $\hat{\Gamma} = \Gamma/\hat{\sigma}$.

We assume two types of particles, the cations with m_1 spherical segments and the single-segment anions ($m_2 = 1$). The molar fractions of the two types are denoted by x_1 and x_2. Since the IL is neutral, we have $x_1 = x_2 = 1/2$. This shows that there is only one independent component and we can use as our thermodynamic degrees of freedom the total ion density, $\rho = (N_+ + N_-)/V$, and the temperature.

Nonelectrostatic Free Energy Terms. The ideal contribution to the free energy is given by

$$\beta a_{\mathrm{Id}} = \log(\rho_{\mathrm{seg}} T^{-3/2}) - 1 \tag{2}$$

where the density of segments is $\rho_{\mathrm{seg}} = \sum_{i=1}^{2} x_i m_i \rho$.

The reference term is proportional to the residual free energy per particle of a Lennard−Jones fluid at the temperature T and density ρ_{seg}, as if all chains were broken into isolated segments:

$$\beta a_{\mathrm{ref}} = \sum_{i=1}^{2} x_i m_i \frac{a_{\mathrm{LJ}}(T, \rho_{\mathrm{seg}})}{T} \tag{3}$$

Here we assumed that all segments are identical Lennard−Jones particles, whose parameters σ and ε are obtained from those of the individual components by means of van der Waals one-fluid theory. The residual Helmholtz free energy for a pure LJ fluid, a_{LJ}, is taken from the correlation proposed by Johnson et al.[45]

The chain term is related to the contact value of the radial distribution function of the reference Lennard-Jones fluid, g_{LJ}^{σ}:

$$\beta a_{\mathrm{chain}} = (1 - \sum_{i=1}^{2} x_i m_i) \log g_{\mathrm{LJ}}^{\sigma}(T, \rho_{\mathrm{seg}}) \tag{4}$$

The contact value g_{LJ}^{σ} is calculated from the expression proposed by Johnson et al.[46]

Electrostatic Free Energy. As stated, the proposed SAFT-MSA model does not incorporate an association term. Instead, following the work of Tan et al.[43] and Gil-Villegas et al.,[42] we represent the effect of Coulomb forces by the closed-form term obtained from a mean spherical approximation of the Restricted Primitive Model. This contribution to the free energy is expressed most simply in terms of the MSA screening parameter (Γ):

$$\beta a_{\mathrm{MSA}} = -\frac{\Gamma(\Gamma + 2/3)}{(\Gamma + 1)^2} \frac{\varepsilon_{\mathrm{ion}}}{T} \tag{5}$$

where

$$\Gamma = \frac{(1 + 2\kappa)^{1/2} - 1}{2} \tag{6}$$

$\kappa = (4\pi\rho\varepsilon_{\mathrm{ion}}/T)^{1/2}$ is the reciprocal of the Debye length, and $\varepsilon_{\mathrm{ion}}$ is the electrostatic energy of two like-charged ions separated by a distance σ.

The correction to MSA called "truncated Γ2 approximation" (TΓ2A) was obtained by Larsen et al. from the procedure called γ ordering;[44] it corresponds to the zeroth-order term in an expansion in powers of the density. The TΓ2A correction amounts to the additional free energy term:

DOI: 10.1021/jp511571h
J. Phys. Chem. B 2015, 119, 5864−5872

$$\beta a_{T\Gamma 2A} = \{[[(1 + 4\Gamma)(4 + \sin(2\Gamma) - 4\Gamma\cos(2\Gamma)]\, e^{-2\Gamma} - 4 - 6\Gamma + 12\Gamma^2 - 40\Gamma^3/3]/128\}(\varepsilon_{ion}/T) \quad (7)$$

Calculation of Derived Thermodynamic Quantities. All calculations were made with the *Mathematica*10.0 software.[47] Explicit expressions for the thermodynamic quantities, such as pressure and chemical potential, were obtained by symbolic differentiation of the free energy models and evaluated numerically afterward.

Specifically, the pressure was calculated from

$$p = \rho^2 T\left(\frac{\partial \beta a}{\partial \rho}\right)_T \quad (8)$$

the chemical potential from

$$\beta\mu = \beta a + \rho\left(\frac{\partial \beta a}{\partial \rho}\right)_T \quad (9)$$

and the reduced entropy per particle from

$$s = -\beta a - T\left(\frac{\partial \beta a}{\partial T}\right)_\rho \quad (10)$$

The critical point was calculated by setting the first two partial derivatives of pressure with respect to density equal to zero, and then solving these two equations for the critical temperature and density.

Liquid−vapor equilibrium densities for each RTIL were calculated numerically. We solved for the equality of pressure and chemical potential in both phases, in temperature ranges that included the simulated results of Rai and Maginn,[18,29] and Hernández et al.[19] For each coexistence under study, in order to calculate the standard boiling-point temperature (T_b), we interpolated the logarithm of the saturation pressure p_{sat} as a function of inverse temperature and solved for the temperature at which p_{sat} = 1 atm. Once T_b was known, the entropy of vaporization at this temperature was calculated as the difference of entropies of the coexisting phases,

$$\Delta s(T_b) = s(T_b, \rho_{vap}) - s(T_b, \rho_{liq}) \quad (11)$$

The corresponding heat of vaporization (per particle) was calculated as $\Delta h(T_b) = T_b \Delta s(T_b)$.

RESULTS

The SAFT-MSA equation has four free parameters: the LJ segments' diameter and energy (σ and ε), the cation size, m_1 and the ionic energy ε_{ion}; this is one parameter less than the five parameters in the soft-SAFT model (σ, ε, m, and the association energy and volume).

To simplify matters, we have taken the cation size as $m_1 = m - 1$, with m being the number of segments per ion pair obtained from the soft-SAFT correlation of Andreu and Vega.[33] We also assumed that the ionic energy has a constant value for each homologous series: One fixed value each for $[BF_4]$, $[PF_6]$, and $[NTf_2]$. This is a reasonable assumption given that each series has the same anion and the same charged group in the cation. To determine the value of ε_{ion} in each series, we focused on the cases with $[C_4mim]$as cation. First, we set σ and ϵ to the values from the respective soft-SAFT correlations. Then, we determined ε_{ion} (as the sole remaining free parameter) by fitting the orthobaric liquid density from simulations of these ILs.[18,19,29] The fitted values correspond in SI units to ε_{ion}= 113.2, 119.2, and 85.9 kJ/mol for the $[BF_4]$, $[PF_6]$, and $[NTf_2]$ series, respectively. The similarity in energy values stems from the fact that the sizes of the anions are very similar.

Next, for the remaining $[BF_4]$ series, we fitted σ and ε to the saturated-liquid density for the cases C_n = 1, 2, and 6 simulated by Rai and Maginn;[29] similarly, for the $[NTf_2]$ cases with C_n = 2 and 6, σ and ε were fitted to the saturated-liquid densities of the corresponding simulations.[18] The fitted values are given in Table 1. The excellent quality of the SAFT-MSA orthobarics is shown in Figure 2: the vapor and liquid branches of the simulated orthobaric are followed closely even at high temperatures. In particular, the saturated vapor density is much lower than that predicted by the soft-SAFT model. Using the parameters just found, we calculated the orthobaric for $[C_4mim][BF_4]$ and $[C_4mim][PF_6]$ for a lower temperature range, 300−800 K, which covers the simulation data of Rane and Errington for these two ionic liquids;[21] Figure 2 shows very good agreement of the results from the SAFT-MSA model with these newer simulation data over quite a wide temperature range.

Table 1. Parameters of the SAFT-MSA Model for Each of the IL Species Studied[a]

IL	σ/Å	ε/kJ mol^{-1}	m_1
$[C_1mim][BF_4]$	3.941	4.0175	2.70
$[C_2mim][BF_4]$	3.978	3.7673	2.97
$[C_4mim][BF_4]$	4.046	3.4932	3.49
$[C_6mim][BF_4]$	4.101	3.2761	4.02
$[C_8mim][BF_4]$	4.167	3.1918	4.55
$[C_4mim][PF_6]$	4.143	3.4685	3.58
$[C_6mim][PF_6]$	4.205	3.5003	4.11
$[C_8mim][PF_6]$	4.638	3.5262	4.64
$[C_2mim][NTf_2]$	4.510	3.7499	5.03
$[C_4mim][NTf_2]$	4.209	3.6188	5.18
$[C_6mim][NTf_2]$	4.331	3.4972	5.34

[a]The common values of the ionic energy for each homologous series correspond to ε_{ion} = 113.2 kJ/mol for $[C_nmim][BF_4]$, 119.2 kJ/mol for $[C_nmim][PF_6]$, and 85.9 kJ/mol for $[C_nmim][NTf_2]$.

After fitting the parameters to the orthobaric data in the manner just described, we predicted standard-pressure densities and compared them with experimental data in a range near room temperature (see Figure 3). For the tetrafluoroborates, the predictions for C_n = 2 and 6 are very accurate over the whole temperature range of the experiments of Seddon et al.[8] For C_n = 8, no simulated orthobaric was available, so we extrapolated σ linearly and ε quadratically to predict the standard-pressure density with good results, as shown in Figure 3. For C_n = 6 and 8 in the $[PF_6]$ series, in order to avoid further fitting, we set σ and ε to the values from their soft-SAFT correlations and then calculated the standard-pressure densities. Again, Figure 3 shows that these predictions are quite good. As for the $[NTf_2]$ family, the prediction of its densities is shown in Figure 3 to be equally successful.

The replacement of the association term by the MSA free energy in the equation of state also improves the prediction of the critical coordinates. Figure 4 shows that the SAFT-MSA model predicts correctly a decrease of the critical temperature, density and pressure as the alkyl-chain size is increased in the $[C_nmim][PF_6]$ homologous series; thus, the model recovers a behavior of RTIL that distinguishes them from nonionic fluids.

DOI: 10.1021/jp511571h
J. Phys. Chem. B 2015, 119, 5864−5872

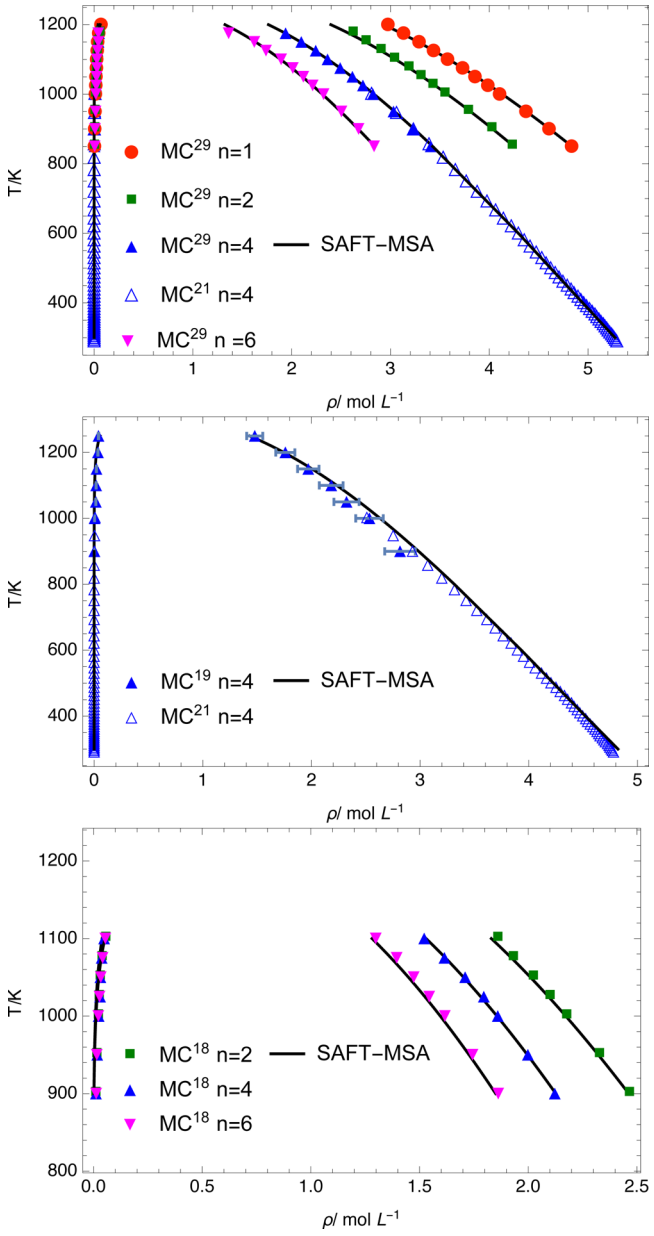

Figure 2. SAFT-MSA model (solid lines) fits very accurately the simulated orthobarics of ionic liquids: (top) $[C_n\text{mim}][BF_4]$ simulated by Rai and Maginn for n = 1, 2, 4, and 6,[29] and by Rane and Errington for n = 4,[21] with their saturated-liquid branches moving systematically to smaller density as the cation size increases; (middle) $[C_4\text{mim}][PF_6]$ simulated by Hernández et al.[19] and by Rane and Errington;[21] (bottom) $[C_4\text{mim}][NTf_2]$ simulated by Rai and Maginn for n = 2, 4, and 6.[18] At this scale, error bars not shown are smaller than the corresponding symbols.

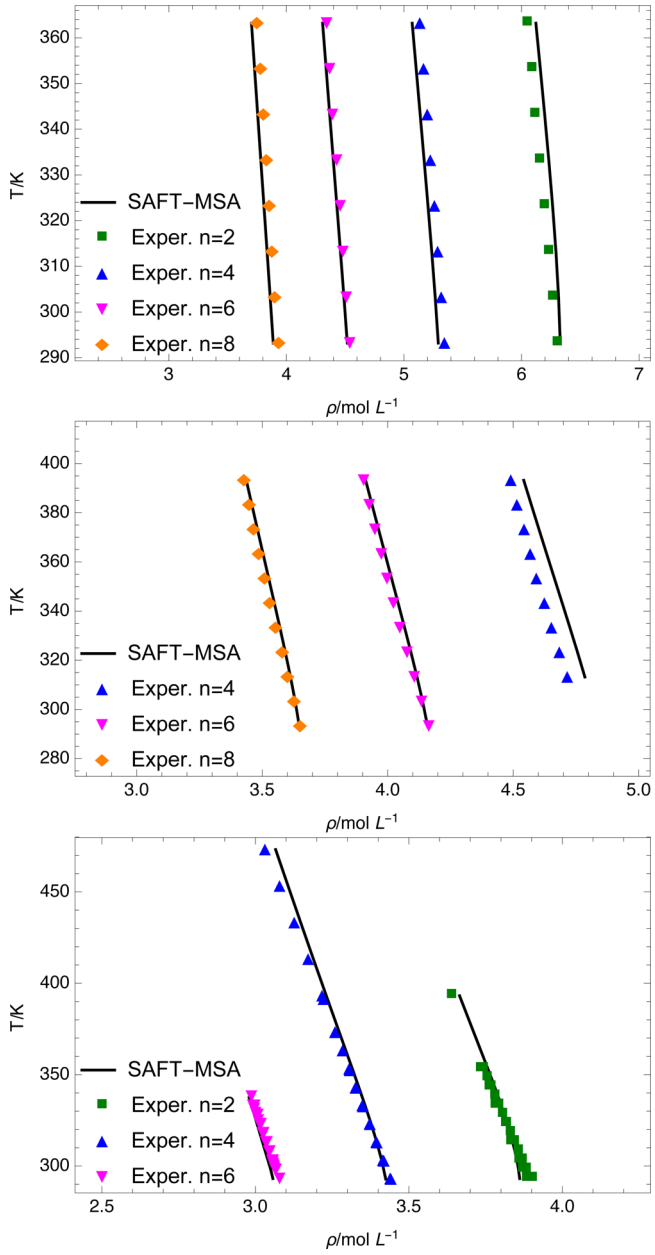

Figure 3. SAFT-MSA model predicts accurately the experimental density of ionic liquids near room temperature at standard pressure: (top) the $[C_n\text{mim}][BF_4]$ family for n = 2, 4, 6, and 8;[8] (middle) the $[C_n\text{mim}][PF_6]$ family for n = 4, 6, and 8;[8] (bottom) the $[C_n\text{mim}][NTf_2]$ family for n = 2, 4, and 6.[12,48−53]

The predictions from the SAFT-MSA equation for T_c and ρ_c agree very well with the simulation results of Rai and Maginn,[29] while that for p_c overestimates the simulated values. Still, it is much closer to them than the prediction from the soft-SAFT model. A similar behavior is found for T_c of the $[C_n\text{mim}][PF_6]$ and $[C_n\text{mim}][NTf_2]$ liquids treated here, that keep the same decreasing tendency with increasing chain length; for the $[NTf_2]$ series, this has been shown in the simulations[18] and actually can be inferred from the bottom panel in Figure 2. Nevertheless, the PC-SAFT calculation of T_c by Paduszynski and Domanska[38] shows a tendency contrary to the simulation results for the $[C_n\text{mim}][NTf_2]$ family. The critical temperature is also predicted, for this family, with good agreement with simulation results; for example, for $[C_4\text{mim}][NTf_2]$ the SAFT-MSA model renders T_c = 1244 K compared with T_c = 1236 K from simulations.[18] Nevertheless, for this family, p_c is overestimated by the SAFT-MSA prediction. As a matter of fact, this error translates into errors in the vapor-pressure: This property is overestimated in the region between T_c and T = 1030 K, attains the exact value at the latter temperature, and is underestimated at even lower temperatures.

The normal boiling point properties as functions of C_n are also much improved. Figure 4 shows that the estimates of T_b, Δs, and Δh from the SAFT-MSA model display the same trend with C_n as in simulations for the $[BF_4]$ family:[18] they all

DOI: 10.1021/jp511571h
J. Phys. Chem. B 2015, 119, 5864−5872

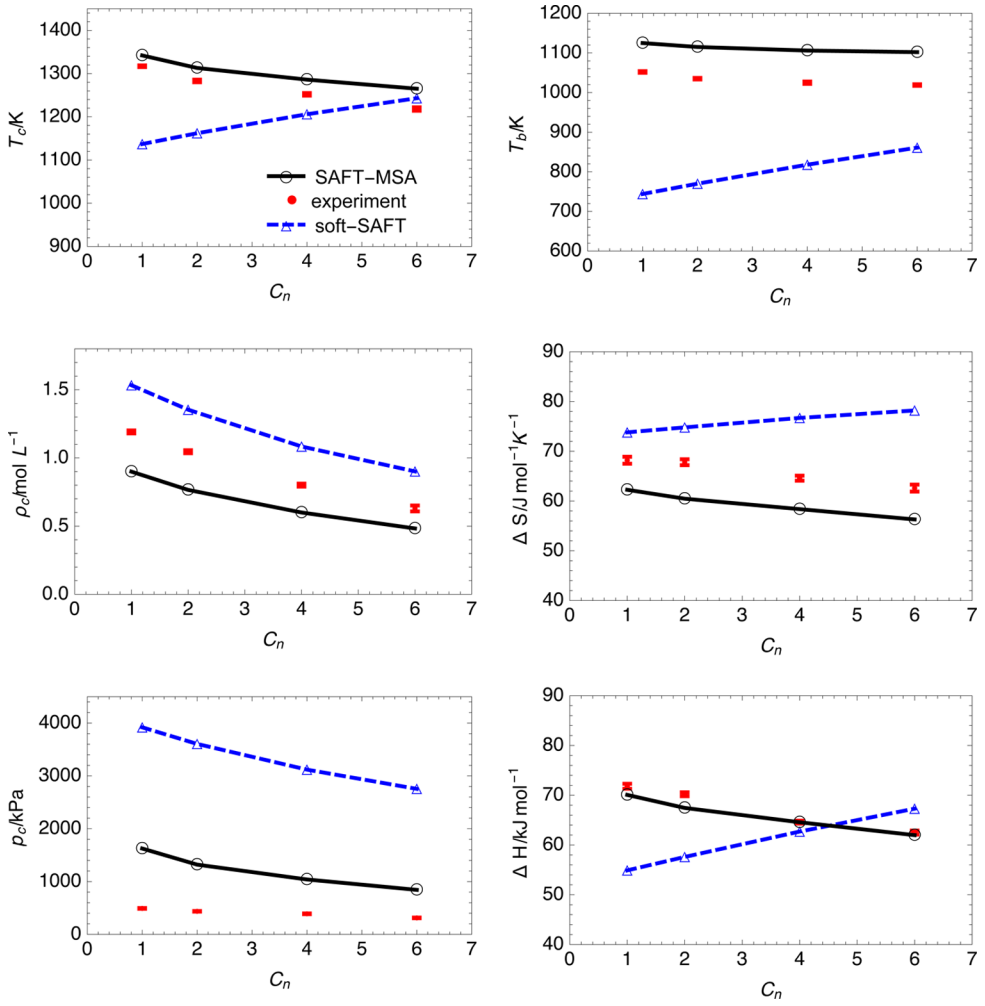

Figure 4. Predictions for the $[C_n\text{mim}][BF_4]$ family from SAFT-MSA and soft-SAFT, as functions of the alkyl-chain size, are compared with the simulations results of Rai and Maginn[29] for: critical temperature, density and pressure (left column), standard boiling-point temperature, entropy and enthalpy of vaporization (right column). All these properties decrease with increasing chain size for the simulations and the SAFT-MSA model; the soft-SAFT model only predicts this decrease for the critical density and pressure.

decrease with increasing alkyl-chain size, in contrast to the increasing trend predicted by the soft-SAFT equation. A small overestimation of T_b is compensated by underestimation of the vaporization entropy Δs, so that the heat of vaporization $\Delta h = T_b\Delta s$ agrees very well with the simulation data of Rai and Maginn.[18] In this regard, Rane and Errington[21] pointed out that the vaporization heat obtained by them (and from experiments) for the family of $[C_n\text{mim}][Tf_2N]$ increases with C_n, contrary to the results of Rai and Maginn using the Gibbs-ensemble Monte Carlo method.[18] We therefore stress the importance of parametrizing equations of state as much as possible in experimental information and to rely on a variety of simulation results. We will return to this point in the Discussion.

In spite of the improvement of the new model over the soft-SAFT results, we considered that going beyond the approximation of the ionic contribution via MSA of the restricted primitive model would be useful. For this reason, we calculated a correction to MSA using the "truncated Γ2 approximation" of Larsen et al.[44] given by eq 7. We found that this correction does not improve the representation of the critical coordinates nor the liquid−vapor equilibria significantly. Also, since the representation of the density is quite good with all three models considered here (soft-SAFT, SAFT-MSA, and SAFT-TΓ2A), we infer that density data near standard pressure and temperature conditions does not provide us with sufficient information to discriminate effectively among different models.

DISCUSSION

From our results, we find that the MSA term for the ionic interaction performs more satisfactorily than the association term in the SAFT methodology, even when the latter approach has more free parameters. Figure 5 shows that both terms contribute to the total free energy in the same qualitative way: they decrease the free energy per particle, and the decrease is larger at higher densities. However, for the same temperature, the MSA term obtained from our model is always more negative than the association term obtained from the soft-SAFT model of Andreu and Vega.[33]

Another difference is that the MSA free-energy term goes as $a_{MSA} \sim \kappa^3 \sim \rho^{3/2}$ for small densities, and hence the density derivative of the pressure diverges at the origin.[42] Care must be taken then when performing low-density expansions.[54] This nonanalytical behavior manifests strongly in the gas, as the isotherms of the free energy and in particular the chemical

DOI: 10.1021/jp511571h
J. Phys. Chem. B 2015, 119, 5864−5872

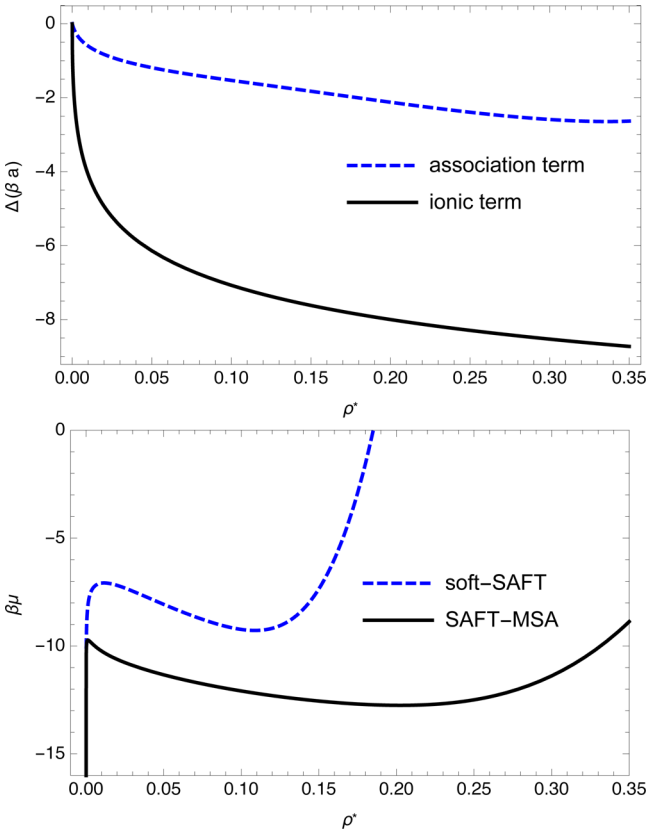

Figure 5. Ionic and association terms contribute to the free energy in the same qualitative way, but the ionic one is larger in magnitude. They are shown at the top panel as functions of reduced density ρ^* at $T^* = 2 \approx 0.7\ T_c^*$ for $[C_4\ mim][BF_4]$. As a consequence (bottom panel), the corresponding chemical potential isotherms for SAFT-MSA and soft-SAFT differ markedly: the ionic term results in a sharper, lower maximum at vaporlike densities and a reduced chemical potential at liquidlike densities. This displaces the orthobaric vapor density toward smaller values.

potential become very sensitive to the precise value of the density in the vapor. This behavior is illustrated in Figure 5.

Another point worth discussing is the variation of the heat of vaporization within an homologous series. The results of Rai and Maginn, shown in Figure 4, indicate a decrease of Δh with increasing C_n.[18,29] Figure 6 shows that, in our parametrization of the SAFT-MSA equation to the $[BF_4]$ series, the heat of vaporization is strongly correlated to the Lennard–Jones energy (when assuming ε is constant); the coefficient of determination $R^2 = 0.998$. This indicates two things: First, that the free parameters may be related more directly to experimentally available data such as the compressibility, or specific and phase-transition heat. Second, that the fitting procedure should include a variety of experimental quantities and not just information from orthobaric densities, since we have shown that the standard-pressure density does not allows one to discriminate reliably between several models.

It is perhaps encouraging that, even if the model parameters are fitted to the saturated-liquid densities, and as can be ascertained from Figure 2, the vapor densities are described fairly well. This means that the SAFT-MSA approach works as a good first approximation to the vapor phase.

Long-standing research shows that modeling the phase behavior of inorganic ionic liquids, such as alkali halides, gives the correct shape for the orthobarics, but a quantitative match

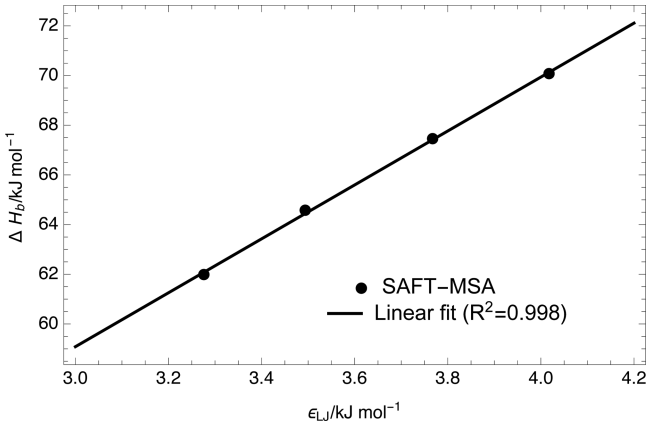

Figure 6. In the SAFT-MSA parametrization of the $[C_n mim][BF_4]$ series, the heat of vaporization at the standard boiling point is linearly correlated to the Lennard–Jones dispersion energy (assuming that the ionic energy ε_{ion} is constant).

calls for a model beyond the RPM that can account for cluster formation.[55,56] This is related to the fact that MSA gives a good starting point for thermodynamics, but does not perform so well in calculating the structure of ionic liquids. The Hyper-Netted Chain (HNC) theory represents an improvement over MSA, but in this case the results must be obtained numerically and not in the form of an explicit equation.[57]

If one is interested in an explicit EOS for ionic liquids, there are other SAFT approaches that are worth exploring. One that we regard as very promising is the Variable Range SAFT equation proposed by Gil-Villegas et al.,[42] originally in the context of electrolyte solutions. This equation allows one to consider explicitly ions with different charges and sizes: SAFT-VR uses as the reference for perturbation a mixture of square-well molecules. Explicit expressions are known for the free energy of this mixture and the values of the various radial distribution functions at contact that are needed. We are not aware of corresponding expressions for a mixture of Lennard–Jones sites with different sizes, so that building an analog EOS for ions with different sizes would require solving this extra step.

CONCLUSIONS

We have shown how the SAFT-MSA equation gives a very good representation of liquid–vapor equilibria properties of ionic liquids. The main difference between the SAFT-MSA and the soft-SAFT EOS is that the new model includes electrostatics explicitly but does not include association, and vice versa.

Specifically, we found excellent agreement with simulated orthobarics for the $[C_n mim][BF_4]$ series,[21,29] for the $[C_n mim][NTf_2]$ series,[18] and for $[C_4 mim][PF_6]$;[19,21] this is a clear improvement with respect to the soft-SAFT results. The prediction of the density at standard pressure near room temperature is also in excellent agreement with experimental data.

The agreement of the critical coordinates (T_c, ρ_c, p_c) with simulation data is improved greatly, being excellent for the critical temperature and density, but the critical pressure still is overestimated. Importantly, the SAFT-MSA model captures correctly the decreasing trends of all critical coordinates with alkyl-chain size, C_n. The decrease of T_c with C_n is a clear improvement over the results from the soft-SAFT EOS and a characteristic behavior of RTIL that models should aim to

DOI: 10.1021/jp511571h
J. Phys. Chem. B 2015, 119, 5864–5872

reproduce. The normal boiling-point temperature, entropy, and latent heat of vaporization are also in very good agreement with the results of the simulations used to parametrize the model.

We agree with Ji et al.[40,41] in supporting IL-modeling strategies that account explicitly for electrostatic contributions to the free energy, since we also obtained best results with the SAFT-MSA equation in comparison with the soft-SAFT model. The reason for this apparent adequacy of introducing the MSA is still not clear. Further research is necessary. It can be said that a full Coulombic formalism does not preclude pair formation, although the MSA approximation is known to fail in dealing with this phenomenon. Currently, we are exploring other schemes that include pairing within a MSA approach.

Why is soft-SAFT still able to recover many thermodynamic properties of RTIL? We have shown that the contribution to the free energy in the soft-SAFT EOS has the same qualitative form as that of the MSA term for the restricted primitive model. Both of them reduce the free energy as density is increased at constant temperature, but the effect is larger for the MSA term; in fact, the MSA term is nonanalytic in the density at $\rho = 0$.

Regarding the application of the SAFT-MSA model, we believe that it would be useful to calculate additional thermodynamic quantities: the thermodynamic coefficients (isothermal compressibilty, thermal expansion coefficient, and heat capacity at constant volume) can be obtained directly by derivation. Comparing the speed of sound and surface tension obtained from the SAFT-MSA model with experimental data would also be strict tests. In addition, the SAFT-MSA model can be generalized in a straightforward way to mixtures containing IL, since it is already modeling a mixture of ions.

While the SAFT-MSA model provides a good equation of state for room temperature ionic liquids, we think that there are still several directions for improvement. To begin, we could improve on the mean spherical approximation in order to obtain a better representation of the RPM contribution to the free energy, for instance by using the hypernetted-chain theory that is used for inorganic molten salts. Going beyond the restricted primitive model may be useful too, in order to quantify the effects of varying the size of cation and anion independently, by applying a SAFT-VR approach to ionic liquids.

AUTHOR INFORMATION

Corresponding Authors

*Phone: +52 (55) 5804-4992. E-mail: ogl@xanum.uam.mx.
*E-mail: jerl71@yahoo.com.
*E-mail: fdr@xanum.uam.mx.

Notes

The authors declare no competing financial interest.

ACKNOWLEDGMENTS

We thank Alejandro Gil-Villegas for useful discussions and acknowledge funding by Mexico's Consejo Nacional de Ciencia y Tecnología (Conacyt), Project No. 105843.

REFERENCES

(1) Rocha, M. A. A.; Santos, L. M. N. B. F. First Volatility Study of the 1-Alkylpyridinium Based Ionic Liquids by Knudsen Effusion. *Chem. Phys. Lett.* **2013**, *585*, 59−62.

(2) Freire, M. G.; Teles, A. R. R.; Canongia Lopes, J. N.; Rebelo, L. P. N.; Marrucho, I. M.; Coutinho, J. A. P. Partition Coefficients of Alkaloids in Biphasic Ionic-Liquid-Aqueous Systems and their Dependence on the Hofmeister Series. *Sep. Sci. Technol.* **2012**, *47*, 284−291.

(3) Calvar, N.; Domínguez, I.; Gómez, E.; Palomar, J.; Domínguez, Á Evaluation of Ionic Liquids as Solvent for Aromatic Extraction: Experimental, Correlation and COSMO-RS Predictions. *J. Chem. Thermodyn.* **2013**, *67*, 5−12.

(4) Louros, C. L. S.; Cláudio, A. F. M.; Neves, C. M. S. S.; Freire, M. G.; Marrucho, I. M.; Pauly, J.; Coutinho, J. A. P. Extraction of Biomolecules Using Phosphonium-Based Ionic Liquids + K_3PO_4 Aqueous Biphasic Systems. *Int. J. Mol. Sci.* **2010**, *11*, 1777−1791.

(5) Llovell, F.; Vilaseca, O.; Vega, L. F. Thermodynamic Modeling of Imidazolium-Based Ionic Liquids with the $[PF_6]$ -Anion for Separation Purposes. *Sep. Sci. Technol.* **2012**, *47*, 399−410.

(6) Bier, M.; Dietrich, S. Vapor Pressure of Ionic Liquids. *Mol. Phys.* **2010**, *108*, 211−214.

(7) Maia, F.; Calvar, N.; González, E.; Carneriro, A.; Rodriguez, O.; Macedo, E. In *Ionic Liquids - New Aspects for the Future*; Kadokawa, J., Ed.; InTech: Rijeka, Croatia, 2013; Chapter 2.

(8) Seddon, K. R.; Stark, A.; Torres, M.-J. Viscosity and Density of 1-Alkyl-3-methylimidazolium Ionic Liquids. *ACS Symp. Ser.* **2002**, *819*, 34−49.

(9) Jacquemin, J.; Husson, P.; Padua, A. A. H.; Majer, V. Density and Viscosity of Several Pure and Water-saturated Ionic Liquids. *Green Chem.* **2006**, *8*, 172−180.

(10) Seki, S.; Tsuzuki, S.; Hayamizu, K.; Umebayashi, Y.; Serizawa, N.; Takei, K.; Miyashiro, H. Comprehensive Refractive Index Property for Room-Temperature Ionic Liquids. *J. Chem. Eng. Data* **2012**, *57*, 2211−2216.

(11) Weiss, V. C.; Heggen, B.; Müller-Plathe, F. Critical Parameters and Surface Tension of the Room Temperature Ionic Liquid $[bmim][PF_6]$: A Corresponding-States Analysis of Experimental and New Simulation Data. *J. Phys. Chem. C* **2010**, *114*, 3599−3608.

(12) Gardas, R. L.; Freire, M. G.; Carvalho, P. J.; Marrucho, I. M.; Fonseca, I. M. A.; Ferreira, A. G. M.; Coutinho, J. A. P. High-Pressure Densities and Derived Thermodynamic Properties. *J. Chem. Eng. Data* **2007**, *52*, 80−88.

(13) Gomes de Azevedo, R.; Esperança, J. M. S. S.; Najdanovic-Visak, V.; Visak, Z. P.; Guedes, H. J. R.; Nunes da Ponte, M.; Rebelo, L. P. N. Thermophysical and Thermodynamic Properties of 1-Butyl-3-methylimidazolium Tetrafluoroborate and 1-Butyl-3-methylimidazolium Hexafluorophosphate over an Extended Pressure Range. *J. Chem. Eng. Data* **2005**, *50*, 997−1008.

(14) Kazakov, A.; Magee, J.; Chirico, R.; Diky, V.; Muzny, C.; Kroenlein, K.; Frenkel, M. NIST Standard Reference Database 147: NIST Ionic Liquids Database (ILThermo); http://ilthermo.boulder.nist.gov/.

(15) Martín-Betancourt, M.; Romero-Enrique, J.; Rull, L. Liquid Vapor Coexistence in a Primitive Model for a Room-Temperature Ionic Liquid. *J. Phys. Chem. B* **2009**, *113*, 9046−9049.

(16) Roy, D.; Maroncelli, M. An Improved Four-Site Ionic Liquid Model. *J. Phys. Chem. B* **2010**, *114*, 12629−12631.

(17) Zhong, X.; Liu, Z.; Cao, D. Improved Classical United-Atom Force Field for Imidazolium-Based Ionic Liquids: Tetrafluoroborate, Hexafluorophosphate, Methylsulfate, Trifluoromethylsulfonate, Acetate, Trifluoroacetate, and Bis(trifluoromethylsulfonyl)amide. *J. Phys. Chem. B* **2011**, *115*, 10027−10040.

(18) Rai, N.; Maginn, E. J. Critical Behaviour and Vapour-Liquid Coexistence of 1-Alkyl-3-methylimidazolium bis-(trifluoromethylsulfonyl)amide Ionic Liquids via Monte Carlo Simulations. *Faraday Discuss.* **2012**, *154*, 53−69.

(19) Hernández, S. G.; Gallo, M.; Alonso, P.; Guirado-Lopez, R.; Dominguez-Esquivel, J. M. Determination of the Vapor−Liquid Equilibrium of Ionic Liquid 1-Butyl-3-Methylimidazolium Hexafluorophosphate using Molecular Simulations. *J. Mol. Liq.* **2013**, *185*, 83−87.

(20) Rane, K. S.; Errington, J. R. Using Monte Carlo Simulation to Compute Liquid-Vapor Saturation Properties of Ionic Liquids. *J. Phys. Chem. B* **2013**, *117*, 8018−8030.

DOI: 10.1021/jp511571h
J. Phys. Chem. B 2015, 119, 5864−5872

(21) Rane, K. S.; Errington, J. R. Saturation Properties of 1-Alkyl-3-methylimidazolium Based Ionic Liquids. *J. Phys. Chem. B* **2014**, *118*, 8734−8743.
(22) Maia, F. M.; Tsivintzelis, I.; Rodriguez, O.; Macedo, E. A.; Kontogeorgis, G. M. Equation of State Modelling of Systems with Ionic Liquids: Literature Review and Application with the Cubic Plus Association (CPA) Model. *Fluid Phase Equilib.* **2012**, *332*, 128−143.
(23) Valderrama, J.; Robles, P. Critical Properties, Normal Boiling Temperatures, and Acentric Factors of Fifty Ionic Liquids. *Ind. Eng. Chem. Res.* **2007**, *46*, 1338−1344.
(24) Valderrama, J. O.; Sanga, W. W.; Lazzus, J. A. Critical Properties, Normal Boiling Temperatures, and Acentric Factors of Another 200 Ionic Liquids. *Ind. Eng. Chem. Res.* **2008**, *47*, 1318−1330.
(25) Wang, J.; Li, C.; Shen, C.; Wang, Z. Towards Understanding the Effect of Electrostatic Interactions on the Density of Ionic Liquids. *Fluid Phase Equilib.* **2009**, *279*, 87−91.
(26) Ji, X.; Adidharma, H. Thermodynamic Modeling of Ionic Liquid Density with Heterosegmented Statistical Associating Fluid Theory. *Chem. Eng. Sci.* **2009**, *64*, 1985−1992.
(27) Vega, L.; Vilaseca, O.; Llovell, F.; Andreu, J. S. Modeling Ionic Liquids and the Solubility of Gases in Them: Recent Advances and Perspectives. *Fluid Phase Equilib.* **2010**, *294*, 15−30.
(28) Lei, Z.; Dai, C.; Chen, B. Gas Solubility in Ionic Liquids. *Chem. Rev.* **2014**, *114*, 1289−1326.
(29) Rai, N.; Maginn, E. Vapor-Liquid Coexistence and Critical Behavior of Ionic Liquids via Molecular Simulations. *J. Phys. Chem. Lett.* **2011**, *2*, 1439−1443.
(30) Tan, S. P.; Adidharma, H.; Radosz, M. Recent Advances and Applications of Statistical Associating Fluid Theory. *Ind. Eng. Chem. Res.* **2008**, *47*, 8063−8082.
(31) Kroon, M.; Karakatsani, E.; Economou, I.; Witkamp, G.; Peters, C. Modeling of the Carbon Dioxide Solubility in Imidazolium-Based Ionic Liquids with the tPC-PSAFT Equation of State. *J. Phys. Chem. B* **2006**, *110*, 9262−9269.
(32) Karakatsani, E.; Economou, I.; M.C, K. tPC-PSAFT Modeling of Gas Solubility in Imidazolium-Based Ionic Liquids. *J. Phys. Chem. C* **2007**, *111*, 15487−15492.
(33) Andreu, J. S.; Vega, L. F. Capturing the Solubility Behavior of CO_2 in Ionic Liquids by a Simple Model. *J. Phys. Chem. C* **2007**, *111*, 16028−16034.
(34) Andreu, J. S.; Vega, L. F. Modeling the Solubility Behavior of CO_2, H_2, and Xe in [C_n-mim][Tf_2N] Ionic Liquids. *J. Phys. Chem. B* **2008**, *112*, 15398−15406.
(35) Llovell, F.; Valente, E.; Vilaseca, O.; Vega, L. F. Modeling Complex Associating Mixtures with [C_n-mim][Tf_2N] Ionic Liquids: Predictions from the Soft-SAFT Equation. *J. Phys. Chem. B* **2011**, *115*, 4387−4398.
(36) Paduszynski, K.; Chiyen, J.; Ramjugernath, D.; Letcher, T. M.; U, D. Liquid-Liquid Phase Equilibrium of (Piperidinium-based Ionic Liquid + an Alcohol) Binary Systems and Modelling with NRHB and PCP-SAFT. *Fluid Phase Equilib.* **2011**, *305*, 43−52.
(37) Paduszynski, K.; Domanska, U. Solubility of Aliphatic Hydrocarbons in Piperidinium Ionic Liquids: Measurements and Modeling in Terms of Perturbed-Chain Statistical Associating Fluid Theory and Nonrandom Hydrogen-Bonding Theory. *J. Phys. Chem. B* **2011**, *115*, 12537−12548.
(38) Paduszynski, K.; Domanska, U. Thermodynamic Modeling of Ionic Liquid Systems: Development and Detailed Overview of Novel Methodology Based on the PC-SAFT. *J. Phys. Chem. B* **2012**, *116*, 5002−5018.
(39) Domanska, U.; Zawadzki, M.; Paduszynski, K.; Królikowski, M. Perturbed-Chain SAFT as a Versatile Tool for Thermodynamic Modeling of Binary Mixtures Containing Isoquinolinium Ionic Liquids. *J. Phys. Chem. B* **2012**, *116*, 8191−8200.
(40) Ji, X.; Held, C.; Sadowski, G. Modeling Imidazolium-based Ionic Liquids with ePC-SAFT. *Fluid Phase Equilib.* **2012**, *335*, 64−73.
(41) Ji, X.; Held, C.; Sadowski, G. Modeling Imidazolium-based Ionic Liquids with ePC-SAFT. Part II. Application to H_2S and Synthesis-gas Components. *Fluid Phase Equilib.* **2014**, *363*, 59−65.
(42) Gil-Villegas, A.; Galindo, A.; Jackson, G. A Statistical Associating Fluid Theory for Electrolyte Solutions (SAFT-VRE). *Mol. Phys.* **2001**, *99*, 531−546.
(43) Tan, S. P.; Adidharma, H.; Radosz, M. Statistical Associating Fluid Theory Coupled with Restricted Primitive Model To Represent Aqueous Strong Electrolytes. *Ind. Eng. Chem. Res.* **2005**, *44*, 4442−4452.
(44) Larsen, B.; Stell, G.; Wu, K. C. Evaluation of a New Self-consistent Approximation for an Ionic Fluid. *J. Chem. Phys.* **1977**, *67*, 530−536.
(45) Johnson, J. K.; Zollweg, J. A.; Gubbins, K. E. The Lennard-Jones Equation of State Revisited. *Mol. Phys.* **1993**, *78*, 591−618.
(46) Johnson, J. K.; Muller, E. A.; Gubbins, K. E. Equation of State for Lennard-Jones Chains. *J. Phys. Chem.* **1994**, *98*, 6413−6419.
(47) Wolfram Research Inc. *Mathematica*, Version 10.0; Wolfram Research, Inc.: Champaign, IL, 2014.
(48) Krummen, M.; Wasswescheid, P.; Gmehling, J. Measurement of Activity Coefficients at Infinite Dilution in Ionic Liquids Using the Dilutor Technique. *J. Chem. Eng. Data* **2002**, *47*, 1411−1417.
(49) Gomes de Azevedo, R.; Esperança, J.; Szydlowski, J.; Visak, Z.; Pires, P.; Guedes, H.; Rebelo, L. Thermophysical and Thermodynamic Properties of Ionic Liquids over an Extended Pressure Range: [bmim][NTf_2] and [hmim][NTf_2]. *J. Chem. Thermodyn.* **2005**, *37*, 888−899.
(50) Esperança, J. M. S. S.; Guedes, H. J. R.; Lopes, J. N. C.; Rebelo, L. P. N. Pressure-Density-Temperature (p-V-T) Surface of [C_6mim]-[NTf_2]. *J. Chem. Eng. Data* **2008**, *53*, 867−870.
(51) Jacquemin, J.; Ge, R.; Nancarrow, P.; Rooney, D. W.; Gomes, M. F. C.; Padua, A. A. H.; Hardacre, C. Prediction of Ionic Liquid Properties. I. Volumetric Properties as a Function of Temperature at 0.1 MPa. *J. Chem. Eng. Data* **2008**, *53*, 716−726.
(52) Tariq, M.; Forte, P. A. S.; Costa Gomes, M.; Canongia Lopes, J. N.; Rebelo, L. P. N. Densities and Refractive Indices of Imidazolium- and Phosphonium-based Ionic Liquids: Effect of Temperature, Alkyl Chain Length, and Anion. *J. Chem. Thermodyn.* **2009**, *41*, 790−798.
(53) de Castro, C. A. N.; Langa, E.; Morais, A. L.; Lopes, M. L. S. M.; Lourenco, M. J. V.; Santos, F. J. V.; Santos, M. S.; Lopes, J. N. C.; Veiga, H. M.; Macatrao, M.; et al. Studies on the Density, Heat capacity, Surface Tension and Infinite Dilution Diffusion with the Ionic Liquids [C_4mim][NTf_2], [C_4mim][dca], [C_2mim][$EtOSO_3$] and [Aliquat][dca]. *Fluid Phase Equilib.* **2010**, *294*, 157−179.
(54) Caillol, J.-M.; Raimbault, J.-L. Sine-Gordon Theory for the Equation of State of Classical Hard-Core Coulomb Systems. I. Low Fugacity Expansion. *J. Stat. Phys.* **2001**, *103*, 753−776.
(55) Pitzer, K. S. Critical-Point and Vapor-Pressure of Ionic Fluids Including NaCl and KCl. *Chem. Phys. Lett.* **1984**, *105*, 484−489.
(56) Pitzer, K. S. Ionic Fluids: Near-critical and Related Properties. *J. Phys. Chem.* **1995**, *99*, 13070−13077.
(57) Hansen, J.-P.; McDonald, I. R. *Theory of Simple Liquids: with Applications to Soft Matter*, 4th ed.; Academic Press: New York, 2013.

DOI: 10.1021/jp511571h
J. Phys. Chem. B 2015, 119, 5864−5872